justification of the use of steady shock polars for a better understanding of truly unsteady flows and for explanatory purposes.

Figure 3a illustrates the regular reflection after transition. The incident shock wave is reflected regularly from the wedge surface. Behind the point of reflection the additional shock wave, which was mentioned earlier, can clearly be seen. The existence of this shock wave was suggested by the multishock polar technique. Its purpose is to support the sudden pressure drop from $P_c$ to $P_d$ (Fig. 2) that takes place at transition. Note that the additional shock wave forms a new triple point on the reflected shock wave of the regular reflection. The slipstream of this triple point collides with the wedge surface and reflects from it in a way which can be termed as "regular reflection of a slipstream." The foregoing discussion concerning the role of the additional shock wave suggests that its strength should be in the vicinity of $P_c/P_d$. Figure 3b illustrates a regular reflection (which was formed after the termination of the inverse Mach reflection) of a *weak* incident shock wave. The above-mentioned additional shock wave is again clearly seen. However, the slipstream emanating from the triple point is probably too weak to be noticed with shadowgraph photography.

## Conclusions

The transition from Mach to regular reflection over a concave cylinder was investigated experimentally. The steady flow $(P,\theta)$ shock polars were used for this unsteady phenomenon in a special way to better understand the process. Although they were used in a truly unsteady flow, it was found that they can predict the phenomenon quite accurately. The use of the multishock polar technique suggested that the transition should go through an inverse Mach reflection and that an additional shock wave should appear after transition to regular reflection behind the reflection point. Both of these predictions were verified experimentally. The experimental study also illustrated the dynamics of the transition from Mach to regular reflection over concave cylinders. Further details on the nature of the inverse Mach reflection can be found in Ref. 4.

## References

[1]Courant, R. and Friedrichs, K.O., *Supersonic Flow and Shock Waves*, Vol. 1, Interscience Publications Inc., New York, London, 1948.

[2]Marconi, F., "Shock Reflection Transition in Three-Dimensional Steady Flow About Interfering Bodies," *AIAA Journal*, Vol. 21, May 1983, pp. 707-713.

[3]Henderson, L.F. and Lozzi, A., "Experiments on Transition of Mach Reflections," *Journal of Fluid Mechanics*, Vol. 68, Pt. 1, March 1975, pp. 139-155.

[4]Takayama, K. and Ben-Dor, G., "The Inverse Mach Reflection," *AIAA Journal*, Vol. 23, Dec. 1985, pp. 1853-1859.

# Visualization of a Forced Elliptic Jet

Ephraim Gutmark* and Chih-Ming Ho†
*University of Southern California*
*Los Angeles, California*

## Introduction

COHERENT structures have been recognized as the dominating feature in free shear layer dynamics.[1-3] Extensive measurements and visualizations have been made about the structures in a circular jet. Recently, Ho and Gutmark[4] found that an elliptical jet with a small aspect ratio (2:1) could substantially increase the entrainment and hence suggested that jets with a small-aspect-ratio asymmetric nozzle could be *an effective passive enhancement device* for entrainment. However, the evolution of elliptical coherent structures are practically unknown, although data about an isolated vortex ring[5,6] or rectangular jet[7,8] with an aspect ratio larger than 5:1 have been reported.

The visualization of coherent structures in an elliptic jet forced in a wide frequency range was presented by the authors at two meetings.[4,9] This range consisted of $1.5\ f_i \geq f_F \geq 0.33\ f_i$, where $f_F$ is the forcing frequency and $f_i$ the initial most amplified frequency in an unforced jet. The evolution of elliptical structures forced at two chosen frequencies is documented in this brief Note. At a low forcing frequency ($f_F = 0.45\ f_i < \frac{1}{2} f_i$), the vortex merging did not occur before the end of the potential core. The vortex merging could be observed about the middle of the potential core at the higher forcing frequency ($f_F = 0.65\ f_i > \frac{1}{2} f_i$).

## Facility

The flow visualization was carried out in an elliptic water jet submerged in a water tank ($737 \times 737 \times 1219$ mm$^3$). The jet had an elliptic nozzle with major and minor diameters of 50.8 mm ($2a$) and 25.4 mm ($2b$), respectively. The shape of the contraction section was circular at the stagnation chamber side and elliptic at the exit. The contours of the contraction in both axis planes were fifth-order polynomials. The diameter of the stagnation chamber was 127 mm. The area contraction ratio was 12.5:1. Honeycomb and screens were installed inside the stagnation chamber to reduce the turbulence level. The water jet was driven by a water pump at a Reynolds number of 14,000, based on the nozzle's major diameter and the exit velocity $U_j$. Forcing was applied by a rotating butterfly valve, which was installed in the bypass branch of the water supply. The initial most amplified frequency $f_i$ in the unforced jet was 6 Hz. The forcing amplitude was about 5% of the jet exit speed. Food color was injected uniformly around the nozzle lip so that the entire vortex ring could be visualized.

## Experimental Results

In the elliptic jet forced at high amplitude $0.05U_j$, the coherent structures were formed at the forcing frequency. Figure 1a shows the flow for the condition $f_F = 0.45\ f_i$, in the view of the major axis plane (the plane containing the major axis of the nozzle). At this forcing frequency, vortices did not merge before the end of the potential core, $x = 5a$. Two features, the lateral deformation and the bending, were distinct from the evolution of the structures in a circular jet. After the vortex ring left the nozzle, it shrank and then expanded in the lateral direction. The necking of the jet column occurred at $x \simeq 1.5a$. The view in the minor axis plane (Fig. 1b) revealed that the structure first expanded and then shrank. Therefore, the elliptic vortex ring switched its axis at $x \simeq 1.5a$ and again at $x \simeq 3a$. Bending of the vortex in the two axis planes were in opposite directions and reached a maximum at $x \simeq a$. The ring became almost flat at $x \simeq 1.5a$ (Fig. 1b). These distortions of nonmerging structures in a jet were very similar to those of an isolated elliptic vortex.[5,6] The measured width $w$ in both axis planes and the maximum deflection $H$ (Fig. 2) agreed well with the numerical results of a single vortex.[6] Obviously, the dynamics of these two flows should be different. However, the matching of the shape distortions implies that the same mechanism, self-induction, governs the deformation of an isolated elliptic vortex[5,6] and the deformation of structures in an elliptic jet.

When the jet was forced at a higher frequency, $f_F = 0.65\ f_i$, vortex merging before the end of the potential core was observed (Fig. 3). Upstream from the merging, the vortices bent and distorted in the lateral direction. However, the defor-

Received April 6, 1984; revision submitted May 24, 1985. 

*Research Associate.
†Professor. Member AIAA.

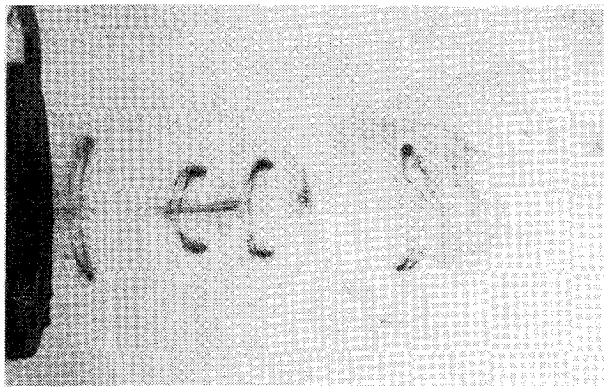

Fig. 1a Side view of the elliptic vortices in the major axis plane ($f_F = 2.7$ Hz $= 0.45 f_i$).

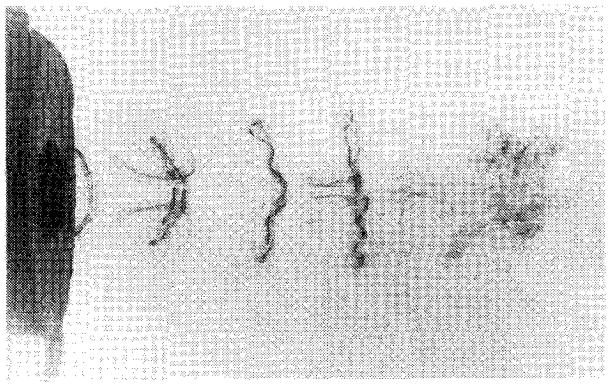

Fig. 1b Side view of the elliptic vortices in the minor axis plane ($f_F = 2.7$ Hz $= 0.45 f_i$).

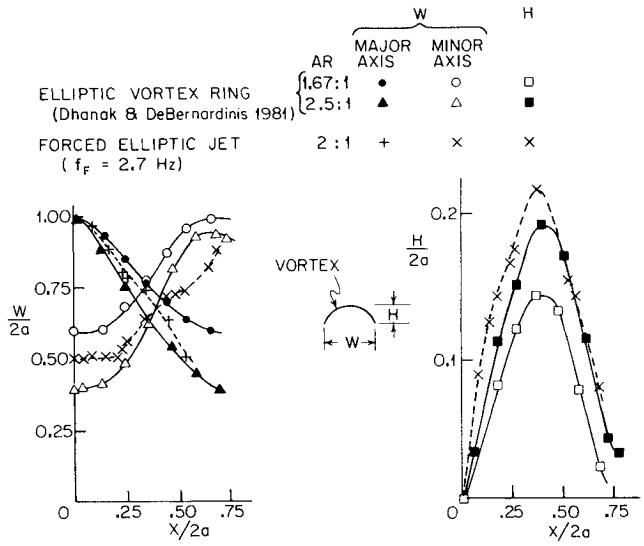


Fig. 2 A comparison between the evolution of the coherent structure in the elliptic jet and isolated elliptic vortex ring.

mation of the downstream vortex in a pair of vortices to be merged was much larger than that of the upstream vortex. The portion of the downstream vortex near the jet minor axis was stretched, and the vorticity was substantially increased. During the merging the corresponding portion of the upstream vortex was therefore induced to move at a high speed and passed through the inner side of the downstream vortex. Conversely, the vorticity of the downstream vortex near the jet major axis side was reduced due to contraction. Hence, the upstream vortex moved slower in the corresponding region. The difference in the induction around the azimuthal direction

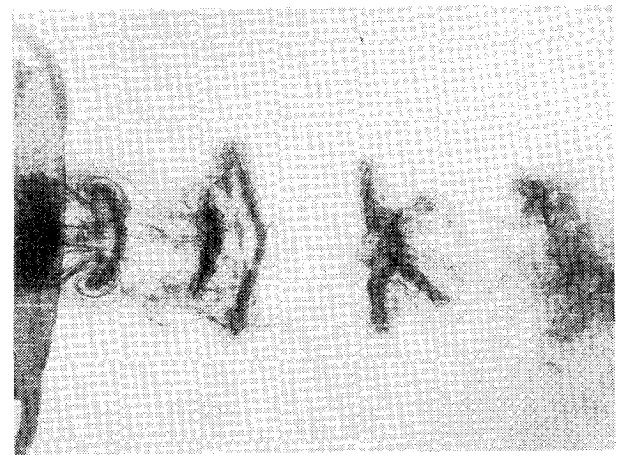

Fig. 3 Side view of the elliptic vortex merging in the minor axis plane ($f_F = 3.9$ Hz $= 0.65 f_i$).

resulted in a vortex merging pattern much different from that in a circular jet with axisymmetric-type vortex coalescence.

## Summary

In an elliptic jet forced at low-frequency range, the vortex merging is suppressed before the end of the potential core. The coherent structure switches its axis due to the self-induction of the asymmetric distribution of vorticity. At higher forcing frequency, the vortex merging is observed. The stretching or contraction around the downstream vortex produces unequal induction on parts of the upstream vortex. Thus, large azimuthal distortion occurred during vortex merging.

## Acknowledgment

This work is supported by the U.S. Air Force Office of Scientific Research under Contract F49620-82-K-0019.

## References

[1]Brown, G. L. and Roshko, A., "On Density Effects and Large Structure in Turbulent Mixing Layers," *Journal of Fluid Mechanics*, Vol. 64, 1974, pp. 775-816.

[2]Winant, C. D. and Browand, F. K., "Vortex Pairing, the Mechanism of Turbulent Mixing Layer Growth at Moderate Reynolds Number," *Journal of Fluid Mechanics*, Vol. 63, 1974, pp. 237-255.

[3]Ho, C. M. and Huerre, P., "Perturbed Free Shear Layers," *Annual Review of Fluid Mechanics*, Vol. 16, 1984, pp. 365-424.

[4]Ho, C. M. and Gutmark, E., "Visualization of an Elliptic Jet," *Bulletin of the American Physical Society*, Vol. 27, Nov. 1982, p. 1183.

[5]Viets, H. and Sforza, P. M., "Dynamics of Bilaterally Symmetric Vortex Rings," *Physics of Fluids*, Vol. 15, Feb. 1972, pp. 230-240.

[6]Dhanak, M. R. and De Bernardinis, B., "The Evolution of an Elliptic Vortex Ring," *Journal of Fluid Mechanics*, Vol. 109, 1981, pp. 189-216.

[7]Trentacoste, N. and Sforza, P., "Further Experimental Results for Three-Dimensional Free Jets," *AIAA Journal*, Vol. 5, May 1967, pp. 885-891.

[8]Krothapalli, A., Baganoff, D., and Karamcheti, K., "On the Mixing of a Rectangular Jet," *Journal of Fluid Mechanics*, Vol. 107, 1981, pp. 201-220.

[9]Gutmark, E. and Ho, C. M., "On the Forced Elliptic Jet," *Proceedings of Symposium of Turbulent Shear Flows*, Karlsruhe, Germany, 1983.